

## T( $t, \alpha$ ) $n, n$ Reaction\*

NELSON JARMIE AND ROBERT C. ALLEN

*Los Alamos Scientific Laboratory, University of California, Los Alamos, New Mexico*

(Received April 25, 1958)

The alpha particle spectra from the T( $t, \alpha$ ) $n, n$  reaction have been measured at a laboratory angle of  $30^\circ$  for triton energies ranging from 0.95 to 2.10 Mev and at laboratory angles of  $30^\circ$ ,  $60^\circ$ ,  $90^\circ$ , and  $120^\circ$  for 1.9-Mev incident tritons. Absolute cross sections are obtained. Analysis of the spectra in terms of a two-stage process involving the formation and breakup of  $\text{He}^5$  is discussed. Evidence for neutron-neutron correlation is observed but no evidence is found for a bound dineutron.

### INTRODUCTION

THE use of accelerated tritons has added an important member to the list of projectiles used in nuclear physics studies. Measurements of the cross sections involved are of theoretical interest in the study of nuclear forces and of practical interest in the development of thermonuclear power. The T+t interaction has been studied by several experimenters.<sup>1-6</sup> The energetically possible interactions for triton energies up to 2 Mev are:

- (1)  $T+t \rightarrow T+t$  (elastic scattering),
- (2)  $T+t \rightarrow \text{He}^6 + \gamma + 12.24$  Mev,
- (3)  $T+t \rightarrow \alpha + n + n + 11.33$  Mev,
- (4)  $T+t \rightarrow \text{He}^5 + n + (11.33 - \epsilon)$   
 $\text{He}^5 \rightarrow \alpha + n + \epsilon$ ,
- (5)  $T+t \rightarrow \alpha + n^2$  (dineutron),

where  $\epsilon$  is the energy associated with the binding of  $\text{He}^5$ . The elastic scattering (reaction 1) has been investigated by Holm and Argo<sup>1</sup> and the present writers.<sup>2</sup> The capture process (reaction 2) has not been studied. Because of the three-body nature of reactions 3 and 4, continuous energy distributions of alpha particles and neutrons are produced. Allen *et al.*<sup>3</sup> measured the alpha particle and neutron spectra at  $90^\circ$  for 220-keV incident tritons and conclude that the reaction proceeds mostly through a statistical three-body breakup. Agnew *et al.*<sup>4,5</sup> studied the neutron and alpha particle yields at several angles for incident tritons in the 1-Mev energy range. Bame and Leland<sup>6</sup> measured the  $0^\circ$  neutron spectrum for 1.48-Mev incident tritons, and conclude that at this energy

reaction 4, the formation and breakup of  $\text{He}^5$  in its ground state, is the most predominant. There is no significant evidence for reaction 5, the formation of a dineutron.

This paper reports on experimental measurements of the alpha-particle spectra from the T( $t, \alpha$ ) $n, n$  reaction at a laboratory angle of  $30^\circ$  for triton energies ranging from 0.95 to 2.1 Mev and at laboratory angles of  $30^\circ$ ,  $60^\circ$ ,  $90^\circ$ , and  $120^\circ$  for 1.9-Mev incident tritons.

### APPARATUS

A collimated beam of tritons, accelerated by one of the Los Alamos 2.5-Mev electrostatic generators, bombards a tritium gas target. The resultant alpha particles are analyzed in a double-focusing magnetic spectrometer and detected in a scintillation counter. A schematic drawing of the apparatus is shown in Fig. 1.

The triton beam is steered and shaped by a steering magnet, an electrostatic deflector, and an alternate-gradient focuser. The beam energy is determined to  $\pm 1.5$  keV by sending the diatomic ( $\text{T}_2^+$ ) beam through a calibrated electrostatic analyser. The tritons pass through circular collimating apertures (25- to 100-mil diameter), enter the gas target through a thin Pyrex foil,<sup>7</sup> and leave through an aluminum foil thick enough to stop completely the  $\text{H}_3^+$  component of the beam. The current is then collected by a Faraday cup containing a "barrier" to suppress secondary electron escape. The reaction fragments leave the gas cell through another glass foil and pass through a defining slit which is located 2 inches from the center of the

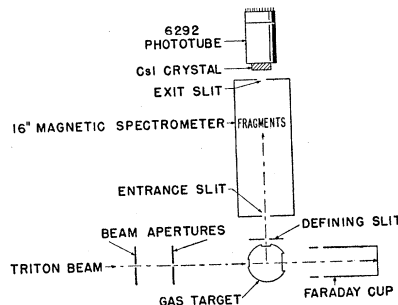


FIG. 1. Schematic drawing of the apparatus: scale and shape are not correct. The indents on the gas target indicate thin foils.

\* Work performed under the auspices of the U. S. Atomic Energy Commission.

<sup>1</sup> D. M. Holm and H. V. Argo, *Phys. Rev.* **101**, 1772 (1956).

<sup>2</sup> R. C. Allen and N. Jarmie, *Phys. Rev.* **111**, 1129 (1958), following paper.

<sup>3</sup> Allen, Almqvist, Dewan, Pepper, and Sanders, *Phys. Rev.* **82**, 262 (1951); **79**, 238 (1950).

<sup>4</sup> W. T. Leland and H. M. Agnew, *Phys. Rev.* **82**, 559 (1951).

<sup>5</sup> Agnew, Leland, Argo, Crews, Hemmendinger, Scott, and Taschek, *Phys. Rev.* **84**, 862 (1951); **79**, 238 (1950); Atomic Energy Research Establishment G/M 68, Proceedings of the Harwell Nuclear Physics Conference, September, 1950 (unpublished).

<sup>6</sup> S. J. Bame, Jr., and W. T. Leland, *Phys. Rev.* **106**, 1257 (1957).

<sup>7</sup> A. Hemmendinger and A. P. Roensch, *Rev. Sci. Instr.* **26**, 562 (1955).

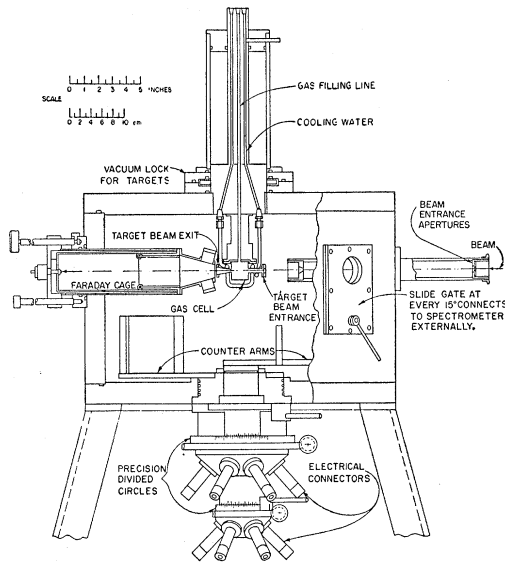


Fig. 2. The 22-inch diameter scattering chamber. Certain minor details have been omitted for clarity.

target and is attached rigidly to the chamber wall. The fragments then pass through three scraping slits and enter the spectrometer through a second defining slit which is located 30 inches from the center of the target and is attached to the spectrometer. Details of the spectrometer and its detector are given in a previous paper.<sup>8</sup>

The entrance apertures, gas target assembly, reaction-product slit system, and Faraday cage are all part of an elaborate 22-inch diameter scattering chamber shown schematically in Fig. 2. Provision is made for two movable counters inside the chamber, which however, were not used in this experiment. External ports are placed every 15° around the chamber to service any exterior equipment, which in this case included the 16-inch magnetic spectrometer. The defining slits, target assembly, and spectrometer may all be moved without breaking the high vacuum through the use of air-lock systems. All the dimensions of the chamber have been checked with precision equipment and are accurate to 1 or 2 mils.

The use of Pyrex glass foils<sup>7</sup> is an important factor in the resolution of the experiment. An average foil is 12 kev thick to 1-Mev protons or about 60  $\mu\text{g}/\text{cm}^2$  (8 micro-inches), although thinner foils were often used. Such foils have successfully held up to 10 cm Hg pressure and have not been tested for the ultimate breaking point. The entrance foil of 100-mils diameter transmits 0.5 to 1  $\mu\text{amp}$  beam (a typical value for this experiment), but eventually becomes brittle because of radiation damage and fails after many days of running. The glass exit foil has no significant beam through it and lasts indefinitely even though it covers a  $\frac{1}{4}$ -inch

diameter hole. The thickness of a foil is measured by observing the threshold of the  $T(p,n)\text{He}^3$  reaction when a proton beam passes through the foil into tritium gas. A "long counter"<sup>9</sup> is used for neutron detection.

#### EXPERIMENTAL PROCEDURE

At a given laboratory angle  $\theta$  and alpha-particle energy  $E$ , the differential cross section for the reaction  $T(i,\alpha)n$  may be written  $\sigma(\theta, E)$ . With customary notation,

$$\sigma(\theta) = \int_E \sigma(\theta, E) dE,$$

and the total cross section is

$$\sigma = \int_{\Omega} \sigma(\theta) d\Omega.$$

In this experiment the relation between  $\sigma(\theta, E)$  and the observed quantities is

$$\sigma(\theta, E) = \sin\theta R Y(\theta, p_m) C_1 C_2 / N n G 2 E_m, \quad (1)$$

where  $\theta$  is the laboratory angle of the alphas;  $R$  is the resolution of the spectrometer and is given<sup>10</sup> by  $p_m / \Delta p_m$  where  $p_m$  is the central momentum of the particles in the spectrometer and  $\Delta p_m$  is the momentum interval corresponding to the detector slit width;  $Y(\theta, p_m)$  is the counting yield in the detector for the momentum  $p_m$ ;  $C_1$  is a correction factor for the distortion of the spectrum caused by the passage of the alphas through the target gas and exit foil;  $C_2$  is a correction factor for the charge exchange of the alphas;  $N$  is the particle density of the target tritons;  $n$  is the integrated number of beam tritons giving  $Y(\theta, p_m)$ ;  $G$  is the geometrical factor<sup>11</sup> and is equal to  $hab/fc$  where  $a$  is the width of the first defining slit,  $h$  and  $b$  are the height and width of the second defining slit at the magnet entrance,  $f$  is the distance of the second defining slit from the center of the target volume, and  $c$  is the distance between the slits; and  $E_m$  is the energy of the alphas at the spectrometer.

Optical methods were used for precise alignment of the chamber, entrance apertures, gas cell, defining slits, and spectrometer in order to insure proper geometrical interrelationships. These methods, aided by the long distance to the second defining slit, resulted in an accuracy of 3 minutes of arc for  $\theta$ , the central angle of the alphas. The maximum included angle of the detected alphas was 2° for the largest slit system.

The resolution  $R$  was measured by observing the width of the scattering edge of protons scattered elastically from a thick copper target.<sup>10</sup> The accuracy of this measurement was at least 2%.

<sup>9</sup> A. O. Hanson and J. L. McKibben, Phys. Rev. **72**, 673 (1947).

<sup>10</sup> Snyder, Rubin, Fowler, and Lauritsen, Rev. Sci. Instr. **21**, 852 (1950).

<sup>11</sup> Worthington, McGruer, and Findley, Phys. Rev. **90**, 899 (1953).

<sup>8</sup> N. Jarmie, Phys. Rev. **104**, 1683 (1956).

The uncertainty in  $Y(\theta, p_m)$  was determined in part by the statistical error in the number of counts observed. Each run was made long enough to give a statistical error of the same order as the other errors in the experiment. Other particles which came through the spectrometer were cleanly separated from the alphas in the detector because of the different sensitivities of CsI to various particles. Background runs were taken by blocking the path between the gas cell and the spectrometer. The background was small except at the lowest alpha energies. The amount of background was reduced by using the thinnest CsI detector crystal consistent with getting the largest signal from the alpha particles.

The correction factors  $C_1$  and  $C_2$  and the determination of the alpha particle energy  $E_m$  are discussed in the next section.

The measurement of  $N$  included determining the temperature and pressure in the gas cell, and the fraction of target atoms in the gas. The gas purity was determined by analyzing samples of the target gas in a mass spectrometer to a precision of 1%. The temperature of the walls of the gas cell was measured to 0.5°C (0.2%) and calculations showed that no correction was needed for local heating of the gas by the beam. The pressure was measured on a 100-mm Wallace-Tiernan gauge, which was in turn calibrated by a high-precision oil and mercury manometer system.<sup>1</sup> The accuracy of the pressure measurement was 0.2%. The usual pressure for the experiment was 5 cm Hg.

The number of incident tritons,  $n$ , was measured with a null type current integrator<sup>12</sup> that was calibrated with a precision current source from the Los Alamos Standards Laboratory. Because of the thickness of the aluminum foil required to stop the  $H_3^+$  component of the beam, multiple scattering of the tritons was significant and the possibility existed that some of the beam might not be collected by the Faraday cage. Extensive precautions were taken and experiments were performed to investigate this possibility and prevent an error in current collection. The effects of changing the pressure in the gas cell, the thickness of the beam exit foil, the energy of the beam, the voltage of the barrier, and the distance of the Faraday cage from the gas cell, which essentially changed the acceptance angle, were determined. The operation of the electric secondary-electron barrier was also tested by adding a magnetic field to the entrance of the Faraday cage. It was found that no corrections for beam collection were needed except for lower triton energies. Rutherford scattering experiments were done with protons and tritons on krypton and argon as a function of energy to determine the correction curve for the multiple-scattering loss of beam particles. The errors introduced varied from 1% at 1.5 Mev to 6% at 0.95 Mev.

<sup>12</sup> R. J. Helmer and A. Hemmendinger, Rev. Sci. Instr. 28, 649 (1957).

The slit dimensions were measured with a travelling microscope and the distances were determined with precision micrometers and calipers. The resultant error in the geometry factor was 0.8%. A typical value of  $G$  used was (for the largest slit system)  $10.41 \times 10^{-4}$  cm.

At the beginning of a day's run, the detector electronics were checked with artificial pulses and the current-integrator calibration was remeasured. As the gas target was filled, a sample was taken to be analyzed. Gas samples were occasionally taken at the end of a day and the degradation of the number of target atoms was found to be about 1%. Frequent readings of pressure, temperature, amplifier setting, and voltages were taken during a run. The beam strength, gas pressure, detector counting rates, and other parameters were varied to test for any experimental inconsistency.

An important test of the accuracy of the experiment was given by observations of proton-proton scattering with this equipment. Measurements of this cross section were taken at intervals throughout the experiment and were within 1.4% of the published values,<sup>11</sup> providing an over-all check on many of the parameters involved, such as  $G$ , pressure and temperature, current integration, proper function of the detector system, and absence of some unusual effect of an anomalous nature. Runs were made with  $D_2$ ,  $H_2$ ,  $CO_2$ ,  $N_2$ ,  $CH_4$ , and He in the gas cell to study the effects of possible contaminants.

## RESULTS

Figure 3(a) shows an example of data observed at 30° in the laboratory for 1.9-Mev incident tritons. The vertical lines represent the statistical errors. The poor statistics near the magnet current of 100 amp are due to lower counting rates necessitated by a high flux of scattered tritons on the crystal. All the sharp peaks can be attributed to known contaminants, and the locations of these products, shown in Fig. 3(b), agree with calculations predicted from known masses. The momentum resolution of these peaks is 0.5%.

The T( $d, \alpha$ ) $n$  reaction comes from a small amount of  $HD^+$  in the beam. Of particular importance is the D( $t, \alpha$ ) $n$  peak at the high-energy end of the spectrum. Previous workers have been unable to separate distinctly these alphas from the  $t-t$  alphas. However, both by the use of deuterium as a target and by the addition of deuterium as a contaminant to a tritium target, the location and shape of this alpha particle peak were determined. From the amount of deuterium in the target gas, as determined by mass spectrographic analysis, the approximate yield of the D( $t, \alpha$ ) $n$  peak was computed. For all the 30° data, the location of this peak was approximately as shown in Fig. 3(b), and merely broadened the high-energy cutoff. At other angles, this contaminant appeared as a sharp peak below the cutoff. It was easy to identify and was used to check the validity of the 30° analysis. Also, at angles

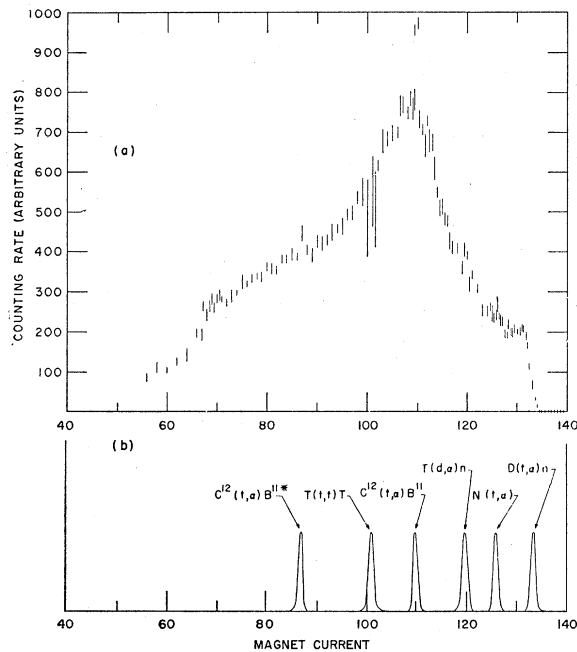


FIG. 3. (a) The alpha particle spectrum from the  $T(t, \alpha)n$  reaction at  $30^\circ$  for a triton energy of 1.90 Mev. The vertical bars represent the statistical errors. (b) The locations of the important peaks of contaminant reactions. The heights are arbitrary. The effect of these contaminants is reflected in the spectrum of Fig. 3(a), as discussed in the text.

other than  $30^\circ$ , the high-energy cutoff of the  $T(t, \alpha)2n$  spectrum agreed exactly with the calculated maximum energy of the alpha. Thus, the calculated maximum was also used as an aid in determining the high-energy cutoff in the  $30^\circ$  data. Further evidence that the shoulders at the high-energy ends of the alpha spectra were not due to a deuterium contaminant is that the yields at the shoulders did not correspond to the known  $D(t, \alpha)n$  excitation function (see Fig. 14).

Smooth curves were drawn through the points after subtracting the contaminant peaks. Values from the smooth curves were then used for the rest of the

TABLE I. Laboratory cross sections for the  $T(t, \alpha)n$  reaction.

$E_t$	$\theta$ (degrees)	$\sigma(\theta)$ (mb/sterad)	Absolute error (%)	Relative error (%)
1.90	30	20.73	4	3
1.90	60	13.6	5	4
1.90	90	5.79	5	4
1.90	120	2.50	7	7
2.10	30	22.1	6	5
2.00	30	21.2	6	6
1.80	30	20.1	5	4
1.70	30	19.2	5	5
1.50	30	17.5	6	6
1.35	30	15.9	5	5
1.30	30	14.8	5	5
1.15	30	12.95	5	5
1.00	30	11.26	6	6
0.95	30	10.86	8	8

calculations. At this point, the curves represented yield,  $Y(\theta, I)$ , versus  $I$ , the magnet current.

Next, corrections for saturation of the magnetic field were applied to give curves of  $Y(\theta, p_m)$  versus  $I'$ , where  $I'$  is the corrected magnet current and is directly proportional to the momentum. This correction, which was determined by measurements made with a proton resonance device, a null type torsion fluxmeter,<sup>8</sup> and known reactions, varied from 0% at a magnet current of 100 amp to 2.3% at 140 amp.

The energy of the alpha particles at the magnet entrance was then computed from  $E_m = kI'^2$ , where  $k$  is a constant determined from known reactions. The final laboratory energy of the alpha particles at the center of the target,  $E$ , was then determined from  $E = E_m + L(E)$ , where  $L(E)$  is the energy lost by the alpha particles in the gas and the exit foil.  $L(E)$  varied from 0.2 Mev for 1.0-Mev alphas to 0.05 Mev for 7.0-Mev alphas. The variation of  $L(E)$  also introduces a correction,  $C_1$ , to the yield. This factor depends on the slope of the energy-loss curve and was 1.15 for 1.0-Mev alphas, 1.05 for 2.0-Mev alphas, and 1.01 for 4- to 7-Mev alphas.

Another important correction was the charge-

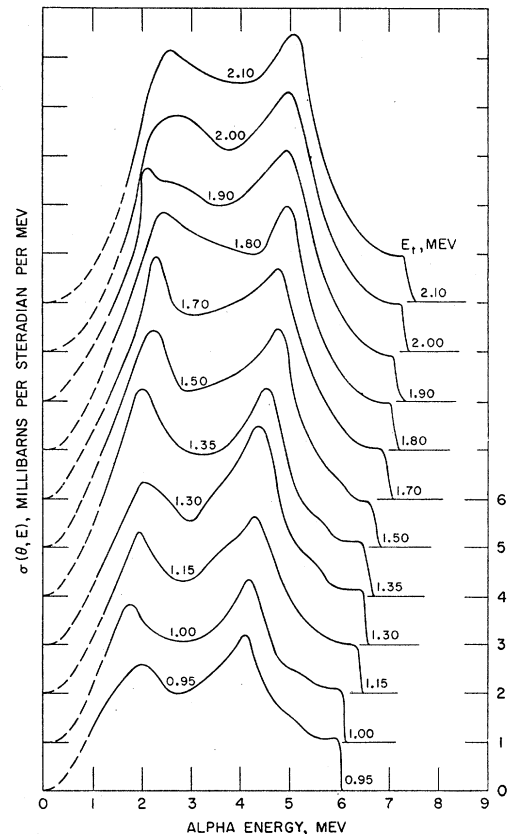


FIG. 4. Experimental alpha spectra (lab system) for various incident triton energies. Lab angle  $30^\circ$ . The scale on the right is used with each curve by matching the zero with each base line.

exchange correction,  $C_2$ . The fraction<sup>13</sup> of total helium ions emerging from the glass foil in a doubly charged state (neutral and singly charged helium atoms were lost) is approximately 0.65 for  $E_m=0.8$  Mev, 0.94 for  $E_m=1.9$  Mev, and 0.99 for  $E_m=6.0$  Mev.

Calculations showed that the multiple scattering of the emitted alpha particles in the gas and foil was significant and its effect had to be determined. The half-width of the multiple-scattering distribution varied from  $0.1^\circ$  to  $0.7^\circ$  depending on the alpha particle energy.<sup>14</sup> The half-angle of the small dimension of the rectangular spectrometer entrance slit, as measured from the exit foil, varied from  $0.05^\circ$  to  $0.8^\circ$  depending on the slit system used. The effects of multiple scattering were studied experimentally by observing protons, tritons, and alpha particles from known reactions with various slit systems. Also, alphas of a given energy from the  $T(t,\alpha)n,n$  spectrum were measured using different slits. All the experimental results indicated that no correction was required. In addition, an extensive graphical analysis using the method of Dickinson and Dodder<sup>15</sup> showed that in all cases the multiple scattering was self-compensating to within 1%. That is, the number of particles scattered out of the collimating system by the foil was just equal to the number scattered in by the foil. Slit-edge scattering effects have also been shown to be negligible.<sup>1</sup>

Figure 4 represents the spectra,  $\sigma(\theta, E)$  versus  $E$ , of the alpha particles observed at  $30^\circ$  in the laboratory for various incident triton energies. The curves were calculated using Eq. (1). The fact that the lower energy peak is larger relative to the higher energy peak in these curves than in the raw data, typified by Fig. 3(a), is primarily due to the division by  $E_m$  in Eq. (1) and

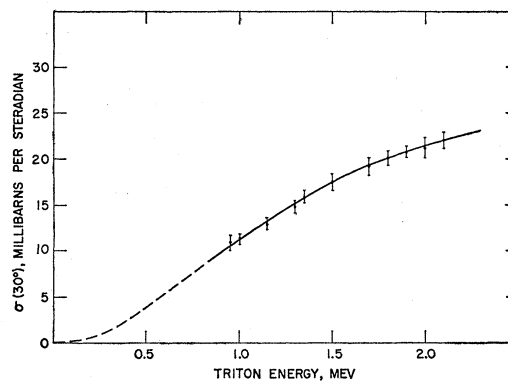


FIG. 5. Lab system excitation function for the  $T(t,\alpha)n,n$  reaction.  $\theta=30^\circ$ . See Table I.

to a lesser extent to the factors  $C_1$  and  $C_2$ . Each spectrum is characterized by two peaks with a shoulder at the high-energy cutoff. The differential cross section  $\sigma(\theta)$  for  $30^\circ$  was obtained at each triton energy by integrating each curve over the alpha particle energy. This excitation function is given in Fig. 5 and Table I. Absence of resonances indicates that there are no levels just above 12-Mev excitation in the compound nucleus,  $He^6$ .

Figure 6 shows the spectra observed at various angles for an incident triton energy of 1.90 Mev. The dashed parts of the curves represent extrapolations. From these data, values of  $\sigma(\theta)$  were determined and are listed in Table I. A plot of  $\sigma(\theta)$  is given in Fig. 7. From this curve the total cross section of the  $T(t,\alpha)n,n$  reaction for 1.90-Mev tritons was found to be  $106 \pm 5$  mb. This result is lower than the  $150 \pm 15$  mb of Agnew *et al.*<sup>5</sup>

The standard deviations for the cross sections are

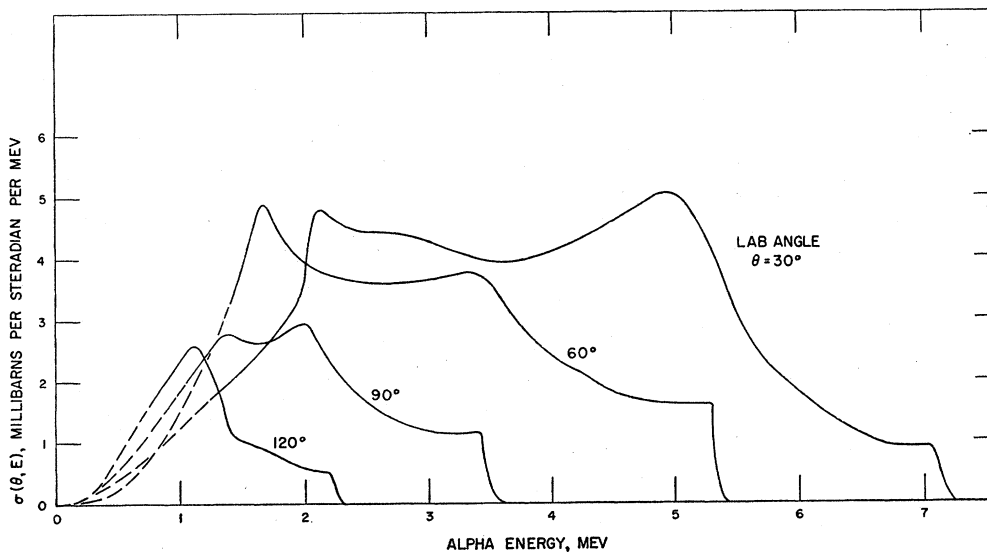


FIG. 6. Experimental alpha spectra (lab system) for various angles.

$E_t=1.90$  Mev.

<sup>13</sup> S. K. Allison and S. D. Warshaw, *Revs. Modern Phys.* **25**, 779 (1953).

<sup>14</sup> H. Bethe, *Phys. Rev.* **89**, 1256 (1953).

<sup>15</sup> W. C. Dickinson and D. C. Dodder, *Rev. Sci. Instr.* **24**, 428 (1953).

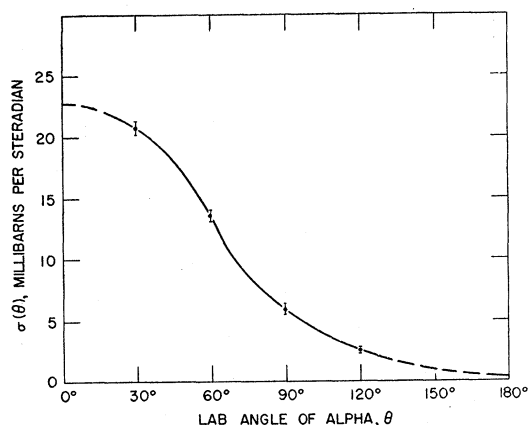


FIG. 7. Angular distribution for the  $T(t, \alpha)n, n$  reaction in the lab system.  $E_t = 1.90$  Mev. See Table I.

formed by the usual composite of the errors in the various experimental quantities that appear in Eq. (1) and the errors in the integrations involved to get  $\sigma(\theta)$  and the total cross section  $\sigma$ . The errors in the specific experimental quantities have been discussed in the section above. The error in finding the area of the various curves graphically, using a planimeter, was no more than 0.5%. There is also the uncertainty involved in extrapolating the initial part of the curves back to zero energy. Assuming nothing unusual happens, this turns out to be from 2 to 4% depending on the particular graph. In the unlikely event that something unexpected happens to  $\sigma(\theta, E)$  at very low energies, the values of  $\sigma(\theta)$  could be in greater error. A random composite of all the errors involved results in the values shown in Table I. These are standard deviations. Also given are the relative errors for the excitation function and the angular distribution. Because the uncertainties common to each set of measurements were small, the relative errors are only slightly less than the absolute errors. The error for any point on the  $\sigma(\theta, E)$  curves is about the same as that for the corresponding  $\sigma(\theta)$ .

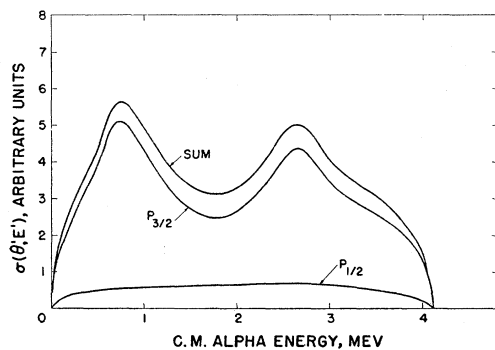


FIG. 8.  $T(t, \alpha)n, n$  reaction, two-stage theory (c.m. system)  $E_t = 1.90$  Mev.

## DISCUSSION

Consider what happens when the reaction proceeds through a two-stage process (reaction 4)<sup>16</sup> the first step being the collision of the two tritons producing a neutron and a  $\text{He}^5$  nucleus and the second step being the breakup of the  $\text{He}^5$  into another neutron and an alpha particle. The following assumptions are made in this calculation: (1) The tritons interact in an  $S$  state. The fact that they are identical particles is also important. (2) The  $\text{He}^5$  nucleus exists either in a  $P_{3/2}$  ground state or a  $P_{1/2}$  excited state. Because  $\text{He}^5$  decays rapidly, both these states are very broad and there is a distribution of binding energies,  $\epsilon$ . (3) The relative probability that  $\text{He}^5$  is formed in one of these states with a particular binding energy is proportion to the respective  $n\text{-He}^4$  scattering cross section.<sup>17</sup>

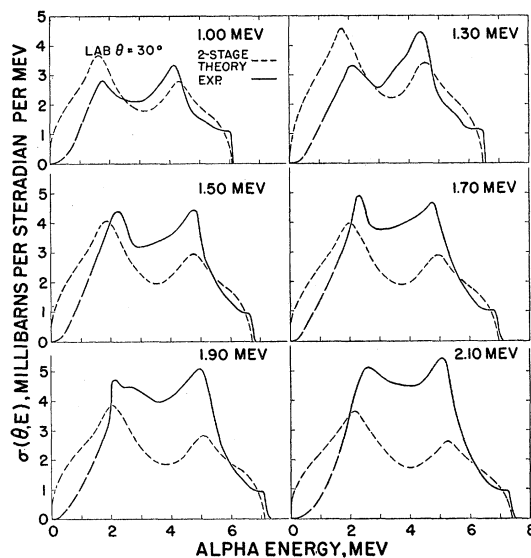


FIG. 9. Theoretical and experimental comparisons for various triton energies. Lab angle  $30^\circ$ .

The calculation then proceeds as follows: It is assumed that the  $\text{He}^5$  is formed with a given angular momentum and binding energy, and the spectrum of final alpha particles is calculated from the mechanics as outlined below. The result then is folded together with the distribution of binding energies deduced from  $n\text{-He}^4$  scattering. These results for the  $P_{3/2}$  and  $P_{1/2}$  states are added to give the final theoretical curve.

The assumption of an  $S$ -state interaction implies that the  $\text{He}^5$  and final alpha particle *angular* distributions are isotropic in the  $t$ - $t$  center-of-mass system. Also, only one direction of motion of the  $\text{He}^5$  nucleus in the  $t$ - $t$  center-of-mass system need be considered to determine the *energy* distribution of the alphas in the  $t$ - $t$  system.

<sup>16</sup> This discussion is a modification and extension of the theory discussed in reference 6.

<sup>17</sup> J. D. Seagrave, Phys. Rev. **92**, 1222 (1953).

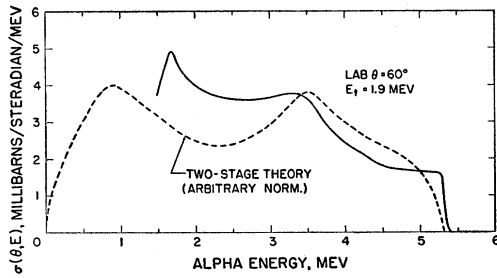


FIG. 10. Theoretical and experimental comparison for 60°.  $E_t=1.90$  Mev.

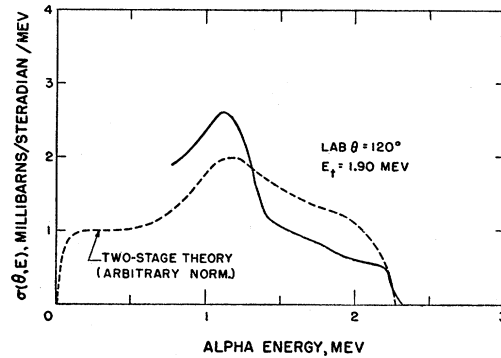


FIG. 12. Theoretical and experimental comparison for 120°.  $E_t=1.90$  Mev.

It can be shown that if the  $He^5$  nucleus is formed in the  $P_{3/2}$  state, the angular distribution of the alpha particles is isotropic in the  $He^5$  center-of-mass system. For a given binding energy  $\epsilon$ , the energy distribution of the alpha particles in the  $t-t$  system thus becomes, for the  $P_{3/2}$  case, a constant between a maximum and a minimum energy, both of which are functions of  $\epsilon$ . However,  $\epsilon$  is a variable, and the final alpha particle energy distribution is a folding or a weighted sum over all possible values of  $\epsilon$ . The weighting function used was the  $P_{3/2}$  component of the total  $n-He^4$  scattering cross section as discussed by Seagrave<sup>17</sup> and Dodder and Gammel.<sup>18</sup>

For the  $P_{3/2}$  formation, the angular distribution of the alpha particles in the  $He^5$  center-of-mass system is proportional to  $1+3 \cos^2\phi$  where  $\phi$  is the angle between the direction of motion of the alpha particle and the direction of motion of the  $He^5$  nucleus in the  $t-t$  center-of-mass system. That is, the angular distribution of the alpha particles is predominantly forward and backward along the direction of motion of the  $He^5$  nucleus, and thus the energy distribution for the  $P_{3/2}$  case, in the  $t-t$  system, is peaked at both the maximum and minimum energies. Again,  $\epsilon$  is a variable, and the final alpha particle energy distribution is a sum weighted by the  $P_{3/2}$  component of the  $n-He^4$  scattering cross section.

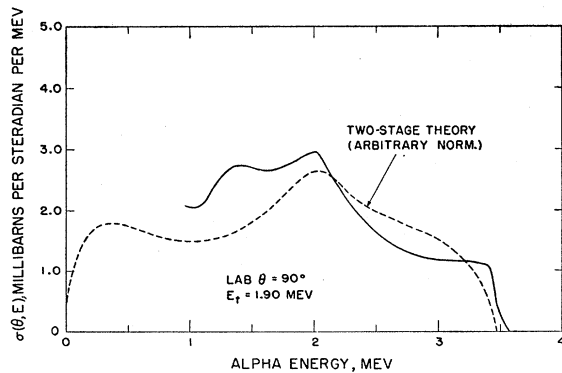


FIG. 11. Theoretical and experimental comparison for 90°.  $E_t=1.90$  Mev.

An example of this calculation, done on an IBM-704 computer, is shown in Fig. 8. It can be seen that the  $P_{3/2}$  ground-state formation is the more predominant. The theoretical curves, transformed to the laboratory system,<sup>19</sup> are compared with some of the experimental results in Figs. 9 through 12. In each case the theoretical curve is arbitrarily normalized to the experimental distribution. These results show that, while there is no striking agreement, some of the general features of the experimental distributions are approximately explained by the two-stage theory. The agreement, particularly for the lower energy peak, is best for the 30° data. The central valleys of the experimental curves are higher than the theoretical curves, implying, perhaps, the existence of some uncorrelated three-body breakup with a purely statistical distribution. In Fig. 13, are shown the experimental distributions transformed to the  $t-t$  center-of-mass system, again with the angular isotropy assumption.<sup>19</sup> It is immediately evident, since

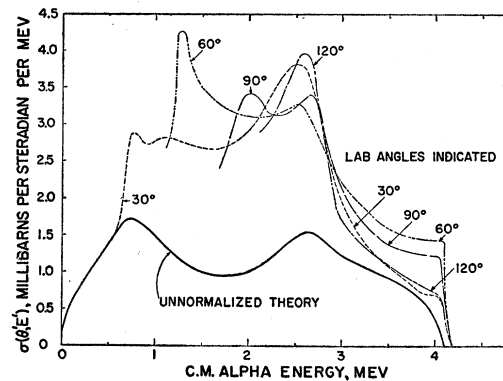


FIG. 13. Center-of-mass presentation of data assuming angular isotropy.  $E_t=1.90$  Mev. The theoretical curve is plotted low for clarity.

<sup>19</sup> The  $S$ -state assumption greatly simplifies the transformation between the laboratory and center-of-mass systems. For example, each laboratory alpha particle energy distribution observed at a laboratory angle  $\theta$  not only transforms to a range of  $t-t$  center-of-mass alpha particle energies,  $E_{\alpha'}$ , but also to a range of center-of-mass angles,  $\theta'$ . The  $S$ -state assumption with the resultant isotropy in the  $t-t$  center-of-mass system, removes the  $\theta'$  dependency.

<sup>18</sup> D. C. Dodder and J. L. Gammel, Phys. Rev. 88, 520 (1952).

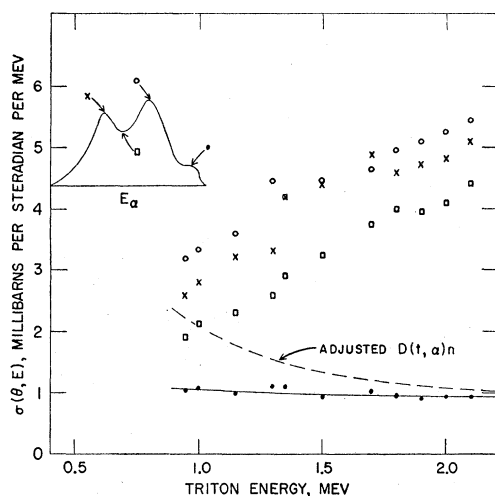


FIG. 14. The variation of alpha particle spectra parameters as a function of bombarding triton energy. Lab angle  $30^\circ$ .

the curves are not alike, that the reaction is not a pure  $s$ -wave interaction. The two-stage theoretical curve is also shown but plotted on a smaller scale for the sake of clarity.

A striking feature in all the experimental curves is the knee near the maximum alpha particle energy. This maximum energy corresponds to the two neutrons going off in the same direction and with the same velocity. An indication that this knee is not due to the  $\text{He}^5$  two-stage process is seen from the variation of the parameters of the distributions as shown in Fig. 14. The excitation function of the knee height has a distinctly different nature than those of the peaks and valley associated with the two-stage process. The increased yield of near-maximum energy alpha particles is probably due to an interaction between the two outgoing neutrons. A graph of the approximate yield of alpha particles of center-of-mass energy 4.04 Mev versus center-of-mass angle is shown in Fig. 15. These values were determined from the distributions given in Fig. 13, reduced by an estimated contribution from the two-stage process. The anisotropy again indicates that the reaction is not a pure  $s$ -wave interaction. The yield of alpha particles due to the neutron correlation is small and amounts to about 1% of the total alpha particle yield. Unfortunately, the peak cannot be resolved well enough to yield any significant information

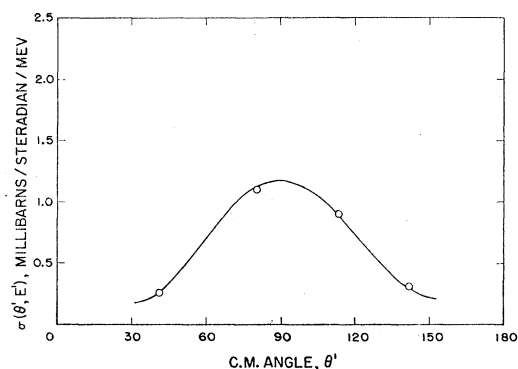


FIG. 15. Center-of-mass angular distribution of alpha particle yield due to neutron correlation. The center-of-mass alpha energy is 4.04 Mev.  $E_t = 1.90$  Mev.

about the  $n$ - $n$  scattering length<sup>20</sup> or the virtual state of the two-neutron system.

A bound dineutron would have caused a narrow alpha particle peak at some energy greater than the end point of the three-body spectrum. This region was carefully searched and no evidence for such a peak was found. An upper limit for the total cross section for the formation of a bound dineutron in this reaction is  $10^{-29}$  cm<sup>2</sup>.

The alpha particle energy spectra are not explained by any one simple process. A simple statistical three-body distribution must be affected by final-state interactions<sup>21</sup> among the particles. As shown by the two-stage  $\text{He}^5$  calculations, the  $P_{3/2}$  and probably the  $P_{1/2}$   $n$ - $\alpha$  interactions are evident. The  $S_{1/2}$   $n$ - $\alpha$  process must also affect the spectra. An  $n$ - $n$  correlation is also indicated. Just how all these processes are related, with possible interference effects, is not clear.

#### ACKNOWLEDGMENTS

We would like to express our appreciation to Wallace Leland for his help during this experiment, particularly for his work on the theory of the two-stage reaction and his data on the early experimental work on the  $T(t, \alpha)n, n$  reaction. Paul Harper and Andrew Lockett also spent much time on the theoretical calculations. Ronald E. Brown and Richard Jacob were of great help at several phases of the work.

<sup>20</sup> Rasmussen, Miller, Sampson, and Gupta, Phys. Rev. **100**, 851 (1955). This article discusses a scattering length analysis in a three-body interaction.

<sup>21</sup> K. M. Watson, Phys. Rev. **88**, 1163 (1952).